SCHMIDT NUMBER DEPENDENCE OF DECAYING PASSIVE SCALAR FLUCTUATIONS IN ISOTROPIC TURBULENCE

P. Orlandi
Dipartimento di Meccanica e Aeronautica
Via Eudossiana 16, Roma Italy
orlandi@kolmogorov.ing.uniroma1.it

R. A. Antonia
Department of Mechanical Engineering
N.S.W., 2308 Australia
meraa@cc.newcastle.edu.au

ABSTRACT

Direct numerical simulations have been carried out for decaying turbulence in a periodic box over a relative large range (0.07 to 7) of the Schmidt number Sc, at a Taylor microscale Reynolds number of about 50. Several small-scale statistics of the passive scalar have been evaluated and compared, when possible, with those from grid turbulence experiments and previous simulations of box turbulence. On the basis of the skewness of the scalar derivatives, the local isotropy of the scalar field appears to be more closely satisfied as Sc increases. The magnitude of the flatness of the scalar derivative is maximum near $Sc \simeq 1$ and decreases rapidly as Sc increases. The extremum seems consistent with the greater dominance of scalar sheets, especially near $Sc \simeq 1$, under the influence of the compressive strain rate. A good collapse of the scalar spectra is observed at sufficiently high wavenumbers when the normalization uses Batchelor scales. The spectra support a k_1^{-1} behaviour, which is first observed when Sc exceeds 1.

INTRODUCTION

The ability to mix scalar contaminants is one of the major characteristics of turbulence. It is therefore not surprising that much effort has been devoted to studying the mechanisms by which turbulent mixing occurs. Much of the impetus for this has come from a wide range of engineering applications wihch require mixing to take place at as rapid a rate as possible. Various types of applications can be cited, irrespectively of whether the molecular diffusivity D of the fluid is much smaller or much larger than the momentum diffusivity or kinematic viscosity ν of the turbulent fluid, i.e. whether $Sc\ (= \nu/D)$ is $\ll 1$ or $\gg 1$.

Prior to the advent of the first direct numerical simulations (DNS) of turbulent flows, the study of the statistics of a scalar, as it is advected by a turbulent flow, was primarily carried out experimentally. The limitations of such an approach are well known, especially when Sc is significantly larger than 1 (e.g. Buch & Dahm, 1996); even when Sc is of order 1, the complexity of obtaining a relatively complete set of information on the small-scale scalar field and its interaction with the small-scale velocity field imposes significant, if not unrealistic, constraints on the experiment. The advantages of DNS in such a case are obvious, notwithstanding the restrictions to relatively low Reynolds numbers and simple flow geometries. There seems to be little doubt that future progress will hinge on exploiting the combined advantages of these two approaches. Quite a number of direct simulations have now been performed for turbulence in a periodic box, which either decays in time or is maintained stationary by forcing at low wavenumbers; we only refer here to those by Kerr, (1985,1990) and by Wang et al., (1999) against which our results have been compared. The simulations have yielded significant insight into the statistics of the small-scale scalar field, its topology and interrelationship with that of the small-scale velocity field (see Buch & Dahm, 1996 who review the major results in the introduction to their paper). Some useful information has also been obtained on the effect of Sc on the scalar field. The overall range of Sc thus far considered in numerical simulations has been too restricted to allow

an accurate assessment of how values of Sc on either side of 1 influence the small scale scalar field, in particular its correlation with the strain rate and energy dissipation rate.

Important theoretical predictions, also based on local isotropy, of the shape of the scalar spectrum were made by Batchelor (1959) for $Sc \gg 1$. Batchelor showed that, for a weakly diffusive scalar, the spectral transfer depends critically on the least principal rate of strain and described the spectrum in terms of γ, the average value of the least principal rate of strain. For $Sc \gg 1$, Batchelor predicted that the three-dimensional scalar spectrum $G(k)$ is given by

$$G(k) = -\left(\frac{\langle\chi\rangle}{\gamma}\right) k^{-1} \exp\left(\frac{Dk^2}{\gamma}\right) \qquad (1)$$

for $k \gg k_K$. $G(k)$ is defined so that $\int_0^\infty G(k)dk = \langle\theta^2\rangle$; $k_K \equiv \eta^{-1}$ is the Kolmogorov wavenumber, $\eta \equiv (\nu^3/\langle\epsilon\rangle)^{1/4}$ is the Kolmogorov length scale, $\langle\epsilon\rangle$ and $\langle\chi\rangle$ are the mean energy and scalar dissipation rates respectively. In the viscous-convective range ($k_K \ll k \ll k_B$), (1) simplifies to

$$G(k) = -\left(\frac{\langle\chi\rangle}{\gamma}\right) k^{-1} \qquad (2)$$

where $k_B \equiv \eta_B^{-1}$ is the Batchelor wavenumber and $\eta_B \equiv (\nu D^2/\langle\epsilon\rangle)^{1/4}$ is the Batchelor length scale. The average value of γ is usually identified with

$$\gamma = -C_B^{-1}\left(\frac{\langle\epsilon\rangle}{\nu}\right)^{1/2} \qquad (3)$$

where C_B is the universal ("Batchelor") constant. Kraichnan (1968) re-examined Batchelor's theory to investigate the effect of fluctuations in the strain rate on the spectrum. The k^{-1} behaviour in the viscous-convective range was unaffected but the Gaussian decay at large k was replaced by a simple exponential.

Confirmation of the k^{-1} behaviour has not been entirely convincing. This is due in part to the inadequate resolution encountered both in measurements and numerical simulations when Sc exceeds 1 but also because the wavenumber range which corresponds to a k^{-1} behaviour invariably starts at wavenumbers smaller than predicted by Batchelor. The fact that Sc has often not been much greater than 1 can be explained by dimensional arguments which only require Sc to be greater than 1 for a k^{-1} behaviour to emerge. Unlike the $k^{-5/3}$ prediction, the k^{-1} behaviour does not require the Reynolds number to be large.

The present DNS data, which cover a significant range of Sc (0.07 to 7), provide information on several aspects of the small-scale scalar field. Results are presented for the effect of Sc on the moments of $\theta_{,i}$ ($\equiv \partial\theta/\partial x_i$). We also compare the θ spectrum with the k^{-1} prediction, given that this behaviour has apparently not previously been observed in simulations of decaying turbulence.

The smallest value of Sc considered here is 0.07 close to the minimum used by Kerr (1985) while the largest value is 7, which allows comparison with available measurements in heated water by Gibson & Schwarz, (1963) and by Clay (1973). A decaying turbulence simulation has certain advantages over forced simulations since most naturally occurring flows are non-stationary or non-homogeneous. The present results should be comparable to those obtained in decaying turbulence downstream of a grid. A comparison with recent measurements ($Pr \simeq 0.7$) obtained in this particular flow (Danaila et al., 2000; Zhou et al., 2000) is provided. The spectrum at $Sc = 7$ is compared with that of Gibson & Schwarz (1963) [$Pr = 7$] also for decaying grid turbulence; note that the latter flow allows $\langle\epsilon\rangle$ and $\langle\chi\rangle$ to be determined with relatively good accuracy.

NUMERICAL METHOD

A finite difference scheme, second-order in space and in time, is used with staggered velocities and with the passive scalar at the same location as u_3. Energy conservation in the inviscid limit is the main reason why a finite difference approach produces results of similar quality to those obtained by pseudospectral methods (for a comparison between finite difference and pseudospectral methods, see Chapter 8 of Orlandi, 1999). The present simulations have been carried out for two resolutions (180^3 and 250^3).

The kinetic energy spectrum, prescribed at $t = 0$, is

$$E(k,0) = \frac{\langle q^2\rangle}{2A}\,\frac{1}{k_p^{\sigma+1}k^\sigma}\exp\left[-\frac{\sigma}{2}\left(\frac{k}{k_p}\right)^2\right],$$

where k_p is the wavenumber at which $E(k,0)$ is maximum, σ is a parameter related to the low wavenumber behaviour, $\langle q^2\rangle \equiv \langle u_i u_i\rangle/2$ is the mean turbulent kinetic energy, here set equal to 1.5 and $A = \int_0^\infty k^\sigma \exp(-\sigma k^2/2)dk$. The simulation has been performed in a cubic box of size equal to 2π; the Reynolds number $Re = (2\langle q^2\rangle/3)^{1/2}/\nu 2\pi$, is 3000 for the coarse

simulation and 3500 for the finer simulation.

For the passive scalar, the simulation was initiated with a random phase spectrum of the same shape as that of $\langle q^2 \rangle$. A certain time interval or relaxation period is needed before $\langle q^2 \rangle$ and $\langle \theta^2 \rangle$ display power-law decay rates. The velocity and passive scalar fields at $t = 10$ are used as the initial conditions for the calculation of a subsequent 10 time units, the scalar transport equation being solved for each value of Sc. The coarse simulations were run at nine values of Sc ($\equiv$ 0.07, 0.15, 0.3, 0.45, 0.7, 1.5, 3, 4.5 and 7), the fine for six ($Sc \equiv$ 0.07, 0.3, 0.7, 1, 3 and 7).

COMPARISON WITH EXPERIMENT AND OTHER SIMULATIONS

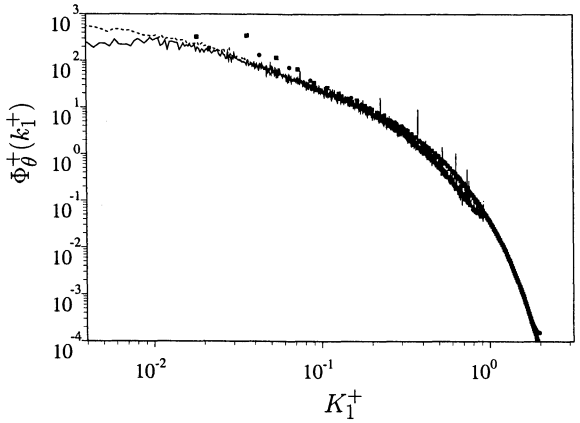

Figure 1: Comparison with measured spectra of θ at $Sc = 0.7$; symbols DNS (• 180^3, ▪250^3), lines measured at (——— R_λ = ...,---- R_λ = ...).

Before discussing the dependence of the passive scalar on Sc, it is worthwhile comparing some basic statistics of the computed velocity and scalar fields with those obtained from previous experiments and simulations of the same type of flow. Ideally, the comparison should be made at the same R_λ, Sc and initial conditions. It is virtually impossible to comply with all these requirements. Here, we restrict ourselves to a comparison with measurements downstream of a grid-heated mandoline (Zhou et al., 2000; Danaila et al., 2000) at approximately the same R_λ ($\simeq$ 50) and Sc ($\simeq$ 0.7). In this flow, $\langle \epsilon \rangle$ and $\langle \chi \rangle$ are known to relatively good accuracy, using

$$\langle \epsilon \rangle = -\frac{d}{dt}\langle q^2 \rangle; \langle \chi \rangle = -\frac{d}{dt}\langle \theta^2 \rangle. \qquad (4)$$

where d/dt is replaced by Ud/dx_1. Different velocities of the oncoming stream were used; at each velocity, R_λ became approximately constant for $x_1/M \geq 40$ (M is the grid mesh size). Figure 1 shows the Kolmogorov normalized spectra of θ compared with those from the present simulations with the two resolutions. In each case, there is good agreement over a substantial portion of the dissipative range. The computed spectra extend to values of k_1^* in excess of 1 whereas the measured spectra extend to significantly lower wavenumbers.

Wang et al. (1999) performed several forced and decaying turbulence simulations; in each case, they evaluated several global quantities related to the velocity and scalar fields. Since they only considered to $Sc \simeq 1$ a higher value of R_λ ($\simeq$ 68) was possible. The integral length scales for the velocity and scalar are related to the three-dimensional energy spectrum $E(k)$ and three-dimensional scalar variance spectrum $G(k)$ via the expressions

$$L_f = \frac{3\pi}{2\langle q^2 \rangle}\int \frac{E(k)}{k}dk \ , \ L_s = \frac{\pi}{2\langle \theta^2 \rangle}\int \frac{G(k)}{k}dk \ .$$

where $\int E(k)dk = \langle q^2 \rangle/2$ and $\int_0^\infty G(k)dk = \langle \theta^2 \rangle$. The Taylor velocity microscale and corresponding scale microscale are given by

$$\lambda_f = \sqrt{\frac{5\nu\langle q^2 \rangle}{\langle \epsilon \rangle}} \quad \text{and} \quad \lambda_s = \sqrt{\frac{6D\langle \theta^2 \rangle}{\langle \chi \rangle}} \ .$$

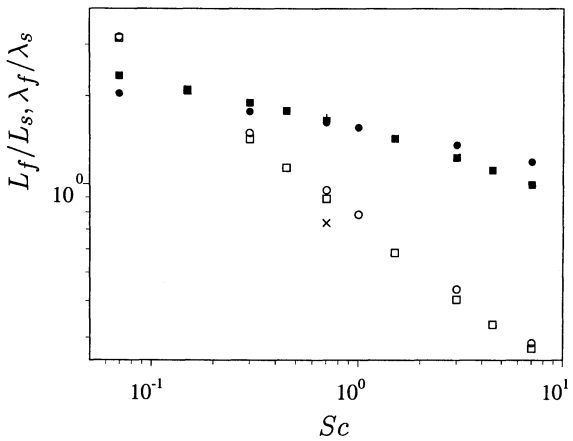

Figure 2: Effect of Sc on integral length scale ratios and Taylor microscale ratios. (○ 180^3, □ 250^3, $t = 20$, △ $t = 30$); open λ, closed L.

Figure 2 confirms that the integral length scale L depend much less on Sc than the hybrid scale λ. The magnitude of the two ratios seems unaffected by the resolution. The dissipation time scale ratio $R \equiv (\langle q^2 \rangle/\langle \epsilon \rangle)/(\langle \theta^2 \rangle/\langle \chi \rangle)$ may also be interpreted as a measure of the life-time of the energy containing eddies relative to that of the scalar fluctuations. Figure 3 indicates that simulations show that this ratio depends on Sc; since $\langle q^2 \rangle/\langle \epsilon \rangle$ is unchanged, the life-time of the scalar fluctuations appears to be

sensitive to Sc. In the grid turbulence experiment of Zhou et al. (2000), R varied slightly with x_1/M; the average value over the range $20x_1/M80$ is about 2.0, in close agreement with the present values. The coarse simulations show a decrease of R with Sc for $Sc > 3$ and this behavior depends on the insufficient resolution of the dissipating range. The closed circles are obtained by the fine simulations at $t = 20$ and even in this case R reaches an asymptote. To fully resolve the dissipation range, the simulations for $Sc = 0.7$ and $Sc = 7$ were continued for another ten time units. Fig. 3 shows that, in this case, there is a shift of the same amount and then it can be asserted that the asymptote is realistic.

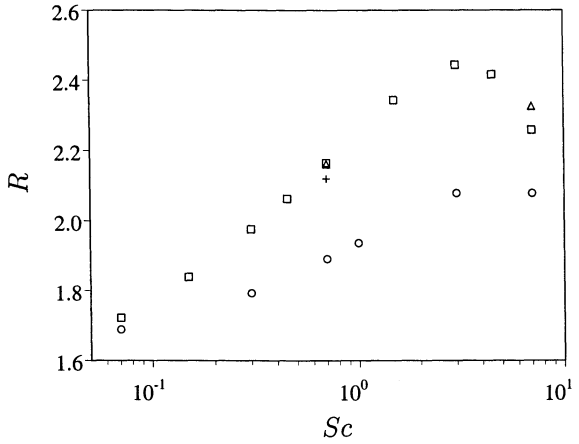

Figure 3: Effect of Sc on R, the time scale ratios (□ 180^3, ○ $250^3, t = 20$, △ $t = 30$); crosses Wang *et al.*.

ISOTROPY AND DEPENDENCE OF SMALL-SCALE PROPERTIES OF THE SCALAR ON SC

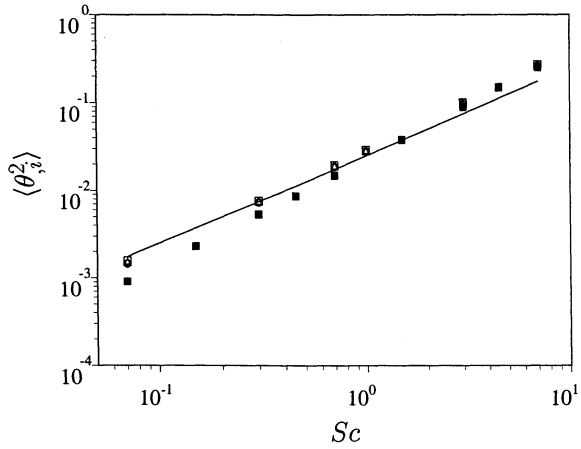

Figure 4: Effect of Sc on the scalar variance of passive scalar gradients solid symbols 180^3, open symbols 250^3 square $i = 1$, diamonds $i = 2$, triangles $i = 3$.

For lack of space we are not presenting the check of local isotropy for the velocity field. To look in more detail at the properties of the scalar field it is interesting to analyse the properties of the statistics of $\theta_{,i}$. In Fig. 4 it turns out that the variances of $\theta_{,i}$ are approximately equal and that these grow linearly with Sc.

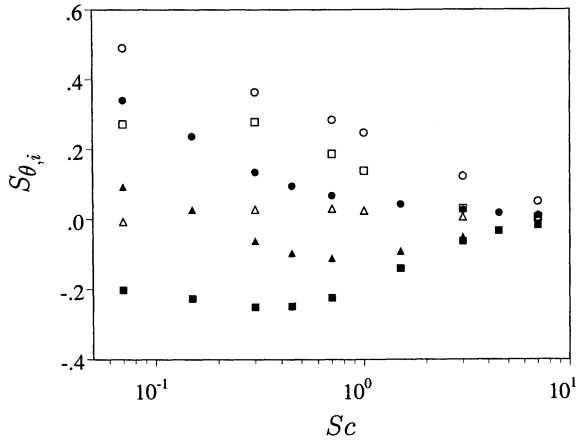

Figure 5: Effect of Sc on the skewness of the passive scalar gradients; legend as figure 4.

The magnitudes of $S_{\theta,i}$ are plotted in Figure 5 as a function of Sc. The non-zero magnitude of $S_{\theta,1}$ is usually interpreted, at least for $Sc \simeq 0.7$, as emphasizing the persistent departure of the scalar from local isotropy. In most flows, $S_{\theta,1}$ is of order 1. A notable exception is grid turbulence in which values very close to zero have been reported. The present DNS value ($\simeq -0.2$) at $Sc = 0.7$ is small compared with the values obtained in shear flows (e.g. Tavoularis & Corrsin, 1981 found that $S_{\theta,1} \simeq -0.95$ and $S_{\theta,2} \simeq 1.1$ in a uniform shear flow with a uniform mean temperature gradient). For the grid turbulence experiment of Zhou et al. (2000), $S_{\theta,1} \simeq -0.18$ at $x_1/M \simeq 40$. At $Sc = 0.7$, the magnitude of $S_{\theta,1}$ is greater than that of $S_{\theta,2}$ or $S_{\theta,3}$. $S_{\theta,2}$ is largest at $Sc \simeq 0.07$.

As Sc increases, the three magnitudes become comparable and are negligible for $Sc = 7$. Given that the skewness of $\theta_{,i}$ is a relatively sensitive indicator of local isotropy, the trend of the data in Figure 5 suggests that local isotropy may be closely approached when Sc is sufficiently large.

The non-Gaussianity of the pdf of $\theta_{,i}$, as reflected by the magnitude of $S_{\theta,i}$, leads to flatness factors of $\theta_{,i}$ which are significantly larger than the Gaussian value of 3. Figure 6 indicates that the three flatness factors are nearly equal, independently of Sc, for the coarse simulation and that there is a weak anisotropy by increasing the resolution, this was found even by Kerr (1985). Both simulation in any case show that $F_{\theta,i}$ is maximum near $Sc = 0.7$. The implication is that the more intense gradients

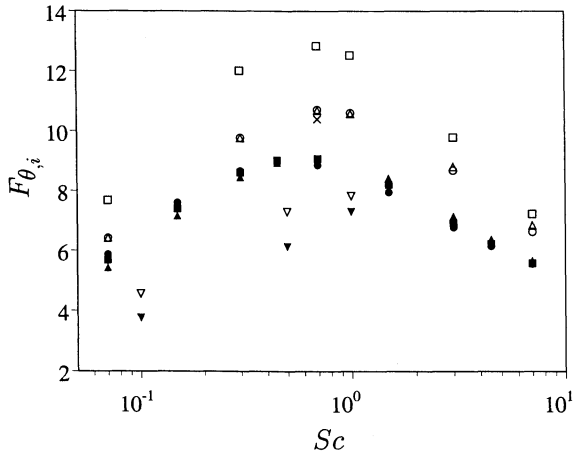

Figure 6: Effect of Sc on the flatness of the passive scalar gradients; legend present results as figure 4, crosses Wang *et al.* inverted-triangles Kerr.

occur near $Sc \simeq 0.7$.

The relatively sharp increase of $F_{\theta,i}$ at small Sc is consistent with the trend implied by Kerr's (1985) values. The smaller values obtained by Kerr most probably reflect the smaller value of R_λ ($\simeq$ 40) and poorer resolution of his forced simulation.

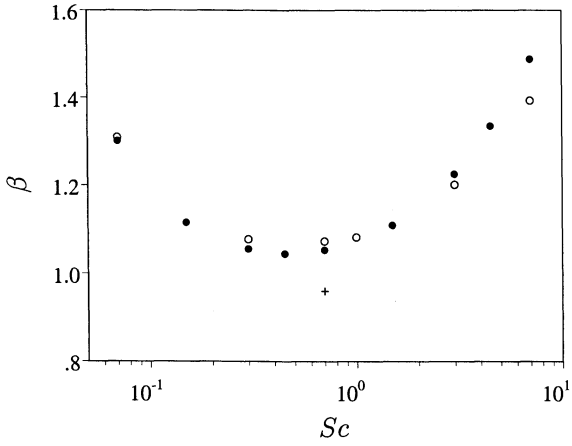

Figure 7: Effect of Sc on β • 180^3, ∘ 250^3 × Wang.

It is of interest to examine whether other small-scale quantities also exhibit an extremum near $Sc \simeq 1$. Kerr (1985) and Wang et al. (1999) considered the ratio β between the production of enstrophy and the production of $\langle\theta_{,i}^2\rangle$, or sometimes palinstrophy, viz.

$$\beta \equiv \left(\frac{\langle\omega_i\omega_j s_{ij}\rangle}{\langle\omega_i^2\rangle\langle s_{ij}s_{ji}\rangle^{1/2}}\right) / \left(\frac{-\langle\theta_{,i}\theta_{,j}s_{ij}\rangle}{\langle\theta_{,i}^2\rangle\langle s_{ij}s_{ji}\rangle^{1/2}}\right) .$$

Figure 7 shows that β is minimum near $Sc \simeq 0.7$, implying that the production rate of $\langle\theta_{,i}^2\rangle$ is largest near $Sc \simeq 0.7$

SCALING OF SPECTRA

As noted in the introduction, the scaling of $\phi_\theta(k_1)$, the one-dimensional spectral density of

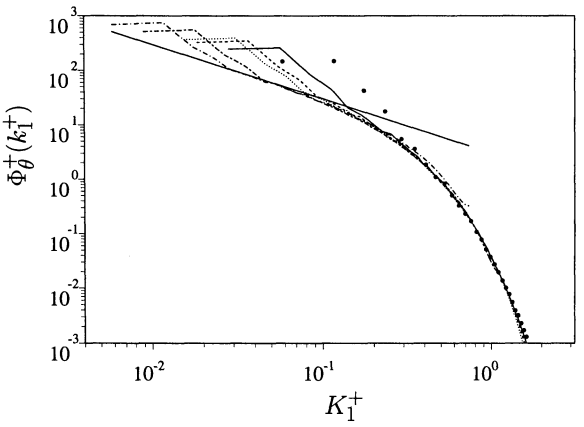

Figure 8: One-dimensional scalar spectra in Batchelor scaling at different Sc for the 250^3 simulations; ∘ Sc = 0.07, ——— Sc = 0.3, - - - - Sc = 0.7, ····· Sc = 1., — - — Sc = 3, —·— Sc = 7, the straight line has the k^{-1} slope.

the scalar, for arbitrary values of Sc is an issue which has received quite a bit of attention. For $Sc \simeq 1$, Kolmogorov-like scaling is appropriate, as shown in Fig. 1. Gibson (1963) pointed out that, irrespectively of Sc, the high wavenumber part of the spectrum should scale on the Batchelor scales $\theta_B = (\langle\chi\rangle/\gamma)^{1/2}$ and η_B The spectrum $\phi_\theta^+(k_1^+)$, where the superscript "+" denotes Batchelor normalization, should therefore depend only on k_1^+ over a range of scales where both ν (or perhaps more relevantly γ) and D are important. The present distributions of $\phi_\theta^+(k_1^+)$, shown in Figure 8, indicate a collapse, at sufficiently large k_1^+. Closer inspection of the high wavenumber portion of these one-dimensional spectra, as highlighted by the linear-log plot reveals that this scaling remains valid up to $k^+ = 1$ for the different simulations. We would like to point out that by increasing Sc the simulation had to evolve for a sufficient long time in order to get a well developed dissipating range. The $k_1^{-17/3}$ behaviour predicted by Batchelor et al. (1969) for $Sc \ll 1$, is not observed in the present $Sc = 0.07$ distribution.

Figure 9 shows a comparison, for $Sc = 7$, between the present spectrum and the temperature spectra measured by Gibson & Schwarz (1963) in decaying grid turbulence and Clay (1973) in the wake of a sphere. As the authors noted, they do however suffer from insufficient spatial resolution; this can be indirectly inferred from the comparison with the present spectrum. It is also the likely reason why a k_1^{-1} range is less evident in the Gibson & Schwarz spectrum than on the present distribution. Strictly, the previous dimensional arguments for a k_1^{-1} behaviour do not require R_λ and Pe to be large (this was also hinted at

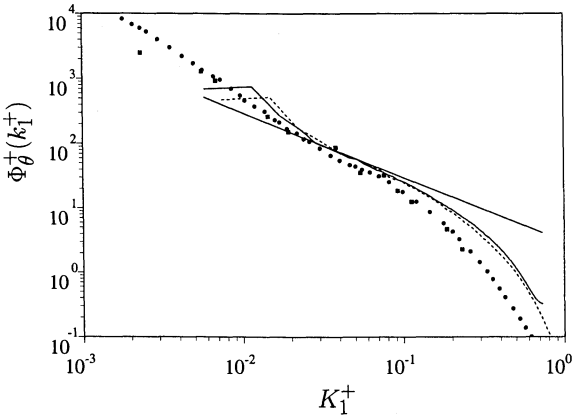

Figure 9: One-dimensional scalar spectra in Batchelor scaling at $Sc = 7$ for the 250^3 simulations (——— $t = 20$, dashed $t = 30$), • Gibson, ▪Clay, the straight line has the k^{-1} slope.

by Batchelor who stressed the role of γ); R_λ is indeed small for all the data in Figure 9.

CONCLUSIONS

The present direct numerical simulations of decaying box turbulence have provided useful insight into the effect of the Schmidt number on the behaviour of the small-scale scalar fluctuations. Perhaps the most significant observation relates to how Sc affects the isotropy of these fluctuations. Since the small-scale velocity field is approximately isotropic, one might expect the small-scale scalar field to behave similarly, in the absence of any extraneous factors such as the presence of a mean scalar gradient. Indeed, second-order and fourth-order moments of $\theta_{,i}$ conform closely with isotropy, almost independently of Sc. This is not the case for third-order moments which seem to conform better with isotropy at the largest Sc ($= 7$). It is now well established that the skewness of $\theta_{,i}$ is a more sensitive indicator of isotropy than even-order moments of $\theta_{,i}$. The approach towards zero of $S_{\theta_{,i}}$ as Sc increases may reflect the increasing gap between the Batchelor length scale and the Kolmogorov length scale.

The scalar spectra exhibit a modest k^{-1} behaviour when Sc exceeds 1. The present decaying turbulence simulation allows direct comparison with grid turbulence measurements ($Pr = 0.7$ and 7), notwithstanding the likelihood that the initial conditions may differ somewhat in each case. Quite reasonable agreement was obtained for $Pr = 0.7$, for the scalar spectra. For $Pr = 7$, there is reasonable agreement with the measured temperature spectrum (Gibson & Schwarz, 1963; Clay, 1973) allowing for the fact that the spatial resolution is poorer for the measurement than in the simulation.

Acknowledgments

RAA is grateful for the support of the Australian Research Council. PO is grateful to MURST for its support.

References

Batchelor, G. K. 1959. "Small-scale variation of convected quantities like temperature in turbulent fluid. Part 1. General discussion and the case of small conductivity", *J. Fluid Mech.*, Vol. 5, pp. 402-407.

Buch Jr., K. A. and Dahm, W. J. A. 1996. "Experimental study of the fine-scale structure of conserved scalar mixing in turbulent shear flows. Part 1. $Sc \gg 1$ ", *J. Fluid Mech.*, Vol. 317, pp. 21-71.

Clay, J. P. 1973. "Turbulent mixing of temperature in water, air and mercury", Ph.D. Thesis, University of California San Diego.

Danaila, L., Zhou, T., Anselmet, F. and Antonia, R. A. 2000. "Calibration of a temperature dissipation probe in decaying grid turbulence", *Expts. in Fluids*, Vol. 28, pp. 45-50.

Gibson, C. H. and Schwarz, W. H. 1963. "The universal equilibrium spectra of turbulent velocity and scalar fields", *J. Fluid Mech.*, Vol. 16, pp. 365-384.

Kerr, R. M. 1985. "Higher-order derivative correlations and the alignment of small-scale structures in isotropic numerical turbulence", *J. Fluid Mech.*, Vol. 153, pp. 31-58.

Kerr, R. M. 1990. "Velocity, scalar and transfer spectra in numerical turbulence", *J. Fluid Mech.*, Vol. 211, pp. 309-332.

Kraichnan, R. H. 1968. "Small-scale structure of a scalar field convected by turbulence", *Phys. Fluids*, Vol. 11, pp. 945-953.

Orlandi, P. 1999. *Fluid Flow Phenomena, A Numerical Toolkit*, Dordrecht, Kluwer Academic Publishers.

Tavoularis, S. and Corrsin, S. 1981. "Experiments in nearly homogeneous turbulent shear flow with a uniform mean temperature gradient. Part 2. The fine structure", *J. Fluid Mech.*, Vol. 104, pp.349-367.

Wang, L-P., Chen, S. and Brasseur, J. G. 1999. "Examination of hypotheses in the Kolmogorov refined turbulence theory through high-resolution simulations", *J. Fluid Mech.*, Vol. 400, pp. 163-197.

Zhou, T., Antonia, R. A., Danaila, L. and Anselmet, F. 2000. "Transport equations for the mean energy and temperature dissipation rates in grid turbulence", *Expts. in Fluids*, Vol. 28, pp. 143-151.